High Performance Commercial Building Systems

Tests of Component-Level Model-Based Fault Detection and Diagnosis Methods using Field Data

June 25, 2004

Peng Xu, Moosung Kim, Philip Haves
Lawrence Berkeley National Laboratory

Subtask 2.3.3 Develop semi-automated, component-level diagnostic procedures
Element 5 – Integrated Commissioning & Diagnostics

Ernest Orlando Lawrence
Berkeley National Laboratory

Table of Contents

ABSTRACT

This paper described the field study of a component-level model-based fault detection method. The method bases on an integrated, life-cycle, approach to HVAC commissioning and performance monitoring. The tool uses component-level HVAC equipment models implemented in the SPARK equation-based simulation environment. The models are configured using design information and component manufacturers' data first. Then it is fine-tuned to match the actual performance of the equipment by using data measured during functional tests of the sort using in commissioning. The fine-tuned model is then used in the operation for the online mointoring and fault detection. This method were tested against the HVAC secondary system in sevearl real commericial buidlings and one experimental facility. The test results and implementation issues are discussed in the paper.

INTRODUCTION

There is a growing consensus that most buildings do not perform as well as intended and that faults in HVAC systems are widespread in commercial buildings. There is a lack of skilled people to commission buildings and commissioning is widely seen as too expensive and/or unnecessary. There is also a lack of skilled people, and procedures, to ensure that buildings continue to operate efficiently after commissioning. One approach to these problems is to wholly or partly automate both commissioning and performance monitoring, using computer-based methods of fault detection and diagnosis (FDD). Component-level FDD, which is the subject of the work presented here, uses a bottom up methodology to detect individual faults by analyzing the performance of each component in the HVAC system (Hyvarinen 1997, LBNL 1999, Haves & Khalsa 2000).

Model-based approaches to fault detection for different HVAC system or sub system have been proposed by various researchers. Benouarets et al. (1994) describe two model-based schemes for detecting and diagnosing faults in air-conditionging systems. They examined their ability to detect water-side fouling and valve leakage in the cooling coil subsystem of an air handling unit. McIntosh et al. (2000) developed a mechanical model for fault detection and diagnosis in chillers. The model was calibrated using data from an operating system and was used in identifying operating faults. Ahn et al. (2001) present a model-based method for the detection and diagnosis of faults in the cooling tower circuit of a central chilled water facility. Faults are detected from deviations in the values of the characteristic quantities from the corresponding values for fault-free operation. The patterns of the deviations are different for each fault, allowing rules to be developed that can be used to diagnose of the source of the fault.

An automated fault detection tool focused on HVAC secondary systems has been developed in this study, based on an integrated, life-cycle, approach to commissioning and performance monitoring. The tool uses component-level HVAC equipment models implemented in the SPARK equation-based simulation environment. The models are configured using design information and component manufacturers' data and then fine-tuned to match the actual performance of the equipment by using data measured during functional tests of the sort using in commissioning. For commissioning, a baseline model of correct operations is normally first configured and adjusted using design information and manufacturers' data. Next, the behavior of the equipment measured during functional testing is compared to the predictions of the model; significant differences indicate the presence of one or more faults. Once the faults have been fixed, the model is fined-tuned to match the actual performance observed during the functional tests performed to confirm correct operation. The model is then used as part of a diagnostic tool to monitor performance during routine operation. In each case, the model is used to predict the performance that would be expected in the absence of faults. A comparator is used to determine the significance of any differences between the predicted and measured performance and hence the level of confidence that a fault has been detected.

A model library has been developed with all the key components in HVAC air distribution systems. The models are able to predict the component performance and detect fault online and offline. The performance of a model-based fault detection tool is critically dependent on the ability of the model to represent the performance of correctly operating equipment in the field. The report presents the results of tests to assess how well the models included in the library can represent the performance of HVAC secondary systems (air handling units and distribution systems).

The tests were performed using data from several buildings in California and from the Iowa Energy Center's test facility. The California buildings include a commercial office building at 160 Sansome Street in San Francisco, the Federal office building at 450 Golden Gate in San Francisco and the Federal office building in Oakland. The results of these tests are presented and discussed. The models were found to be capable of representing the performance of correctly operating equipment and detecting several types of incorrect operation. Implementation issues are also discussed.

SUPPORTING SOFTWARE TOOL

A toolbox of software that supports the model based fault detection methods has been developed. The toolbox includes a preprocessor, a steady state detector, a comparator, and a framework to support the data flow and analysis.

Since the model-based fault detection tools proposed here can be used in both commissioning and routine operation. As it is shown in Figure 1, in the software tool, during the commissioning phase, design information and manufacturer's performance data are first used to calibrate the model. Functional test data taken during start-up tests are then used to detect any pre-existing faults. Once remedial work has been performed, the tests are repeated to confirm that the faults have been corrected. Once the test results are considered satisfactory, the test data are used to recalibrate the model for use in the on-line monitoring phase. The predictions of the recalibrated model are compared with routine operating data, in order to detect any faults that may arise during subsequent operation.

Figure 1 Data flow of the model-based component-level FDD method

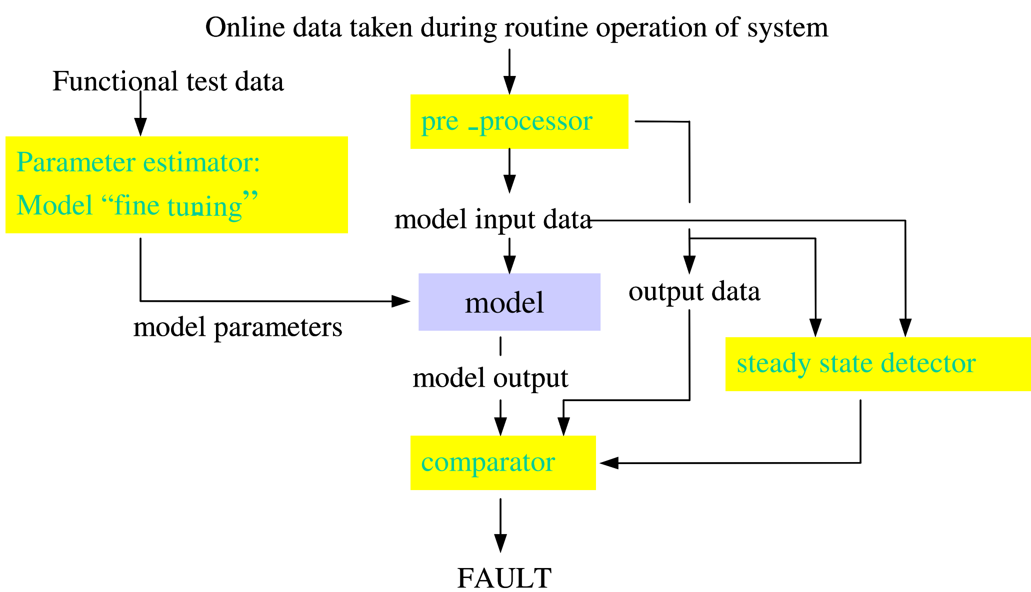

MODEL AND THEIR DATA REQUIREMENT

The field tests are focused on three components model in the model library (Xu and Haves, 2001) : the mixing box model, the VAV fan system model, the coil/valve model. A brief view of these models is presented here. More detailed information is given in Xu and Haves (2001). The models addressed in this paper are listed in Table 1, along with the measurements that are assumed to be available as inputs to the model.

Table 1. Inputs and outputs of models

	Inputs	Outputs	Parameters
Mixing box	• control signal to damper actuators • outside air temperature • return air temperature • outside air humidity • return air humidity	• mixed air temperature • mixed air humidity • N.B. Since mixed air temperature is often not measured and mixing is often incomplete anyway, supply air temperature (corrected for temperature rise across the supply fan) is often used as a proxy for mixed air temperature when the coils are inactive.	• Installed return damper leakage (0-1) • Installed outside air damper leakage (0-1) • Outside air fraction when damper position is 0.5 • Polynomial constants of curve fitting outside air fraction as a function of damper position
VAV fan system	• fan speed (assumes variable speed drive) • volumetric air flow rate	• supply fan: supply duct static pressure • return fan: room pressure (may be assumed to be ~0.1inH_2O if not measured) • fan pressure rise • fan power	• fan curve constants • resistance characteristic constants • constant to calculate fan efficiency • fraction of motor heat loss entering air stream • pressure-fan speed constant • fan efficiency • maximum fan efficiency • motor efficency
Coil/valve system	• control signal to valve actuator • water inlet temperature • air inlet temperature • air inlet humidity	• leaving air temperature • leaving water temperature • leaving air humidity	• External heat exchange area • Internal heat exchange area • Constant of heat exchange of external surface • Constant of heat exchange of internal surface • Valve authority, • Valve Leakage parameter • Mass flow rate for open valve • Mass flow rate with closed valve • Inherit valve resistance ratio (valve resistance divided by valve resistance at full open)

One issue in modeling for fault detection is that some degree of imperfect operation may be tolerated in practice (e.g. leakage of valves or dampers) and so must be included in models that ostensibly represent correct operation.

Mixing box

Prediction of the mixed air temperature and humidity in an air handling unit involves estimating the outside and return air fractions and then performing heat and moisture balances on the mixed air stream. Prediction of the air-flow fractions based on the control signals to the actuators that position the dampers is impractical because (i) the return air and mixing plenum pressures change with fan speed and (ii) it is difficult to estimate air-flow resistances in mixing boxes. This said, the behavior in the middle of the operating range is relatively unimportant compared to the behavior at each end of the operating range. An empirical approach to modeling the airflow fractions has therefore been adopted.

At the commissioning stage, when only design information is available, the range of acceptable behavior is modeled. A 3:1 gain variation is used by default; when the damper position is 50%, the permitted upper limit of the outside air fraction is 75% and the lower limit is 25%. The maximum acceptable deviations from 0 and 100% outside air fraction at each end of the operating range, which are determined by the leakage in the dampers, should be specified by the designer, based on the performance required and manufacturer's data. Note that leakage can arise from imperfections in the dampers themselves, the incorrect installation in the duct or from a mismatch between the ranges of operation of the damper and its actuator. Once the mixing box has been commissioned, the results of the functional test can be used to fit a polynomial to the measured variation of the outside air fraction with the control signal to the damper actuator.

VAV fan system

The model treats VAV systems that have fans with variable speed drives. Fan performance is modeled by using the fan similarity laws to normalize the volumetric flow rate, V, pressure rise, Δp_{fan}, and power, P, in terms of the rotation speed, n_{fan}. Over the limited range of normalized flow used in normal operation, the relationship between fan pressure rise and volumetric flow rate can be approximated using a constant term and a squared term. The constant term is the pressure rise extrapolated to zero flow rate, which is proportional to the square of the rotation speed, and the squared term corresponds to the pressure drop inside the fan. The model is written in terms of total pressure (i.e. static pressure plus velocity pressure) since energy losses are directly related to changes in total pressure. The pressure rise across the fan is then:

$$\Delta p_{fan} = k_{fan} n_{fan}^2 - C_{fan} V^2 \qquad (1)$$

where k_{fan} and C_{fan} are empirical constants that will be determined initially from manufacturer's head curve data or from field measurements of flow rate, pressure rise and rotation speed.

The pressure rise across the fan is balanced by the system pressure drop, which consists of the pressure drop in the other air handling unit (AHU) components and in the distribution system components. The pressure drop, Δp_{res}, can also be represented by two terms. For the supply fan subsystem, the first term is the total pressure in the supply duct at the position of the sensor used to control the fan speed, p_{stat}. The second term represents the pressure drop through the AHU and distribution system components, $C_{res}V^2$. The total pressure at the static pressure sensor is the sum of the static pressure and the velocity pressure ($\rho V^2/2A^2$), where ρ is the density and A is the cross sectional area of the duct.

$$\Delta p_{res} = p_{stat} + (C_{res} + \rho/2A^2)V^2 \qquad (2)$$

For the return fan subsystem, p_{stat} is the measured or assumed pressure in the occupied space and appears as a negative term in Equation 3, since a positive pressure in the space reduces the fan pressure rise required. The correction for the velocity pressure in the room is very small and can be ignored.

$$\Delta p_{res} = -p_{stat} + C_{res} V^2 \qquad (3)$$

Combining the equations for the pressure rise across the fan and the system pressure drop yields:

$$p_{stat} = k_{fan} n_{fan}^2 - (C_{fan} + C_{res} + \rho/2A^2)V^2 \qquad (4)$$

which is used to predict the measured static pressure in the duct (or the pressure in the space) from the fan speed and the air flow rate. If the airflow rate is not measured but there are measurements of fan power and fan pressure rise, the airflow rate can be estimated directly if the combined efficiency of the motor and fan, η, is known from catalog data or one time measurement:

$$V = \eta p / \Delta p_{fan} \qquad (5)$$

If the fan power is measured but the fan pressure rise is not, the airflow rate can be estimated by solving:

$$V = \eta p / (k_{fan} n_{fan}^2 - C_{fan} V^2) \qquad (6)$$

Note that it is not possible to determine the flow rate and the efficiency independently. The flow rate must be measured in order to determine the efficiency. The efficiency can be assumed to be constant over the range of operation or it can be approximated by a quadratic relationship in the normalized flow rate, V/n, about the maximum value, η_{max}:

$$\eta = \eta_{max} - E(V/n - V_{max}/n)^2 \qquad (7)$$

Finally, when assessing the thermal performance of the mixing box and coils, it is useful to be able to use the measurement of supply air temperature as a proxy for the mixed air temperature or the off-coil air temperature. In a draw-through system, this requires correcting for the temperature rise, ΔT, across the fan, which can be estimated from the pressure rise and the efficiency:

$$\Delta T = \Delta p/\eta\, \rho c_p \qquad (8)$$

A summary of the data requirements for VAV fan system and the data source is given in Table 2.

Table 2. Requirements for VAV fan system data

Inputs	Requirement	Source
Fan speed	Required	Measured
Volumetric air flow rate	Required	Measured or calculated using eq.5 or eq.6
Supply duct static pressure	Required	Measured
Room pressure	Required	Measured
Fan pressure rise	Required if air flow rate unknown or can not calculated from fan power	
Fan power	Required	Measured
Fan/motor efficiency	Required if airflow rate is unknown or fan pressure rise is unknown	Catalog data or calculated using Eq.7 based on one time measurement
Fan temperature rise	required for mixing box calibration	Measured or calculated using Eq. 8

Coil and valve sub system

Heating coils typically have one or two rows of tubes and are essentially cross-flow devices. Cooling coils typically have four or more rows and are essentially counterflow devices. They may provide dehumidification as well as sensible cooling and the surface in contact with the air may then be partially or completely wet. Most heating coils, at least in climates where there is no risk of freezing, and all cooling coils are controlled by varying the flow rate of water through the coil. Coils in VAV systems also experience variable air flow rate. The challenges in coil modeling are to treat the variation in surface resistance with flow rate and to treat partially wet operation.

The most common fault to be detected in either heating or cooling coils is fouling of the heat exchange surface, either on the air or the water side. In order to detect fouling when it occurs, it is only necessary to model full load operation. However, in order to be able to predict loss of capacity at peak load before it occurs, it is necessary to model part load operation as well.

In the coil model, the coil is divided into a number of discrete sections along the direction of fluid flow. In each section, heat and mass balance equations are established for each fluid, together with rate equations describing the heat and mass transfer. If the dew point temperature of the air is lower than the metal surface temperature, that section of the coil is treated as dry. If not, the water condensation rate is assumed to be proportional to the difference between the humidity ratio of the bulk air stream and the humidity ratio of saturated air at the temperature of the coil metal surface. The coefficient of proportionality is determined by assuming the value of the Lewis Number is unity. The sections that make up the coil are linked together by associating the fluid inlet conditions of one section with the outlet conditions for the adjacent upstream section.

SPARK then solves the resulting set of coupled equations. Although the computational burden of the new coil model is significantly greater than that of the ASHRAE Toolkit models, the model is robust, and it has the additional advantage of being a suitable starting point for a dynamic cooling coil model.

The most common faults associated with control valves are: leakage, stuck valve/actuator, actuator/valve range mismatch, and unstable control. In order to detect these faults, it is more important to model the valve behavior at each end of the operation than in the middle. However, as discussed in the Coil section, it is desirable to be able to predict the part load performance of coils in order to anticipate loss of peak capacity before it occurs. Since the water flow rate through a coil is not generally measured in HVAC systems, it is necessary to treat the behavior of the control valve at intermediate flow rates by modeling its inherent and installed characteristics in order to predict the water flow rate through the coil.

The water flow rate is a function of the valve position, the flow rate through the valve when fully open and the leakage. The flow characteristic is assumed to be parabolic, which is an adequate and convenient approximation to the modified equal percentage characteristic used in most control valve intended for this application.

FIELD TEST SITES

In total four sites were selected for testing. At each site, the field test follows the same procedures: 1) collecting HVAC system design information; 2) Construct the models using design information or catalog data; 3) Calibrate the model using performance data; 4) Determine whether the performance model is good enough for online monitoring.

Iowa Energy Center

Iowa Energy Center's Energy Resource Station (ERS) is a real building but is operated as an experimental facility. The HVAC system at the ERS consists of three variable-air-volume (VAV) air-handling units: a matched pair that serve test rooms and a single unit that serves the occupied spaces. The data used here are from one of the matched pair (AHU_A).

The models in the library were tested using data that are expected to be representative of the measurements that would be obtained from functional tests on a well-controlled system. The measurements were made by ERS staff under carefully controlled conditions using well-established procedures. One advantage of the ERS is that the sensors are regularly calibrated, so that sensor error is unlikely to confound the experimental results. The data presented here are the results of two sets of step tests on the mixing box, coils and fans. All the step tests were open loop tests that were conducted by overriding the feedback controller and adjusting the output signal from minimum to maximum, and then from maximum to minimum, in a predetermined series of small steps. Relatively large numbers of steps were employed in order to determine which particular steps provide the most useful information. It is anticipated that the tests used in practice will use fewer steps.

160 Sansome Street, San Francisco

The building in which the tests were performed is a 100,000 ft^2 commercial office building located in downtown San Francisco. The building has two chillers and one main air-handling unit. The AHU consists of a mixing box, a cooling coil, a supply fan and a return fan. The return fan is controlled so as to maintain a fixed pressure in the building. There is no heating coil in the air-handling unit and the heating load is satisfied by reheat coils in the terminal boxes in the exterior zones of each floor. Approximately half of the floors of the building are equipped with constant flow terminal boxes and the other half are equipped with variable-air-volume terminal boxes.

This building was built in 1960's and relatively little information regarding the mechanical system is available. The number and location of sensors is more representative of what is usually found in HVAC systems in commercial buildings. The supply and return airflow rates are not measured, neither is there a measurement of coil water leaving temperature or flow rate. The catalogy data of the components are not avaible.

Offline data was collected from a series of functional tests. Functional tests were performed on the mixing box and the supply fan. The tests were designed to be performed while the building was occupied, which required the tests to be relatively short and have limited impact on indoor thermal comfort. For each sub-system, both open loop and closed loop tests were performed. In the closed-loop tests, a number of different operating points were achieved by changing the controller set-point. Open-loop functional testing was conducted by overriding the controller and forcing the output to the desired positions. To determine the hysteresis of the actuators, step tests in both directions were performed for the mixing box dampers.

Chabot Space and Science Museum

Chabot Space & Science Center is an 86,000-square-foot, state-of-the-art science and technology education facility on a 13-acre site in the hills of Oakland, California. The coolingplan had a 230 Ton centrifugal chiller with variable pumping chilled water loop. There are eight air-handling units located in the roof use chilled water to condition outside air and provide air circulation throughout the entire facility. Seven of them are Single duct variable air volume air handling units and one is constant volume unit. A DDC control system installed by Yamas in May 2000 provides indoor comfort control. Operation data set were collected from site over one month period in summer. AHU6 is the air hundling unit where the model were tested.

FIELD TEST RESULTS

Mixing box

Iowa Energy Center

The mixing box model is a generic model and no design information is required to construct the initial model. The results for the mixing box test at Iowa Energy Center are shown in Figure 2. The measurements of the outside, return and mixed air temperatures and the demanded position of the damper actuators are shown in Figure 2A. Since there is relatively poor mixing in most mixing boxes, the supply air temperature, corrected for the rise across the supply fan using Equation 8, is used as a proxy for the mixed air temperature. The maximum mixed air temperature is very close to the return air temperature and the minimum mixed air temperature is very close to the outside air temperature, indicating that leakage is small. Figure 2B is a comparison of the measured mixed air temperature and the mixed air temperatures corresponding to the 3:1 gain range described above and shown in Figure 2. The measured values lie between the permitted upper and lower limits, except when the demanded position of the damper is ~10%, when the damper fails to open significantly, in part because of hysteresis. Figure 2C shows the X-Y plot of the outside air fraction versus the damper position. Figure 2D shows the simulated mixed air temperature and outside air fraction using two polynomials for the damper operation, one for opening and one for closing.

Figure 3 shows examples of fault detection using measurements of mixing box performance made when the return air damper had been fixed in the closed position. The outside and exhaust air dampers were closed in 10% steps and then opened in 20% steps, as shown in Figure 3A. In automated commissioning, such faults can be detected during the functional testing phase if the measured mixed air temperature lies outside the permitted range, as can be seen in Figure 3B. During routine operation, the fault can be detected by comparing the measured and simulated mixed air temperatures (Figure 3C) or the measured and simulated outside air fractions (Figure 3D).

Fan systems

160 Sansome Street, San Francisco

The initial values of the two constants of the fan model itself, was obtained using manufacturer's performance data. Altough the manfucture ceased to exist anymore, the old catalog data was collected through a collective search effort with local cosultant companies.

For this building, some changes in procedure were required because certain measurements or information that were available at the experimental facility were not available at the field test site. As is often the case in commercial buildings, there was no measurement of supply or return airflow. Without an estimate of the airflow, it is not possible to predict the performance of fan and coils. However, in this building, the pressure rise and power were measured for both fans, so the airflow rates could be estimated.

The fan model was calibrated using the fan curve provided in the old catalog. Then the calibrated model was used to simulate the real performance. Since there is no air flow rate measurement on site. The fan power was used to back calculate the air flow (eq. 5). Figure 4 shows the results for the supply and return fans. Figure 4A, 4C, 4E are for the supply fan and 4B, 4D, 4F are for the return fan. Because the building was occupied at the time, the tests cover only a limited part of the operating range. Figure 4A shows the different phases of the supply fan test. Figure 4B is the comparison of the measured pressure rise across the supply fan and the pressure rise predicted by the calibrated model. The model predicted is about 0.5 inWg higher than measured in the building. The supply fan performance is perhaps degraded over time and did not performance as well as it was designed. There are greater fluctuations in the simulated pressure than in the measured pressure and the major cause is fluctuations in the fan speed. After talking with the building operator, it emerged that the supply fan has a problem with slipping belts, which leads to oscillation of the supply fan speed and power. This is corroborated by the estimated parameter values of the fan model; the efficiency of the supply fan is 5% lower than that of return fan, even though both fans are similar models from the same manufacturer and are the same age.

Figure 4B,D,F shows the corresponding results for the return fan. Unlike the supply fan, the calibrated model generally agrees well with measured data for pressure rise. Over the limited range of operation that could be covered in the tests, the model is able to achieve a good fit to the measured data for both the supply and return fans. This should allow the detection of faults such as increased resistance due to fouling of coils or filters or a change in the fan pressure rise *vs.* speed relationship due to incorrect wiring of the fan motor following electrical repairs. Changes in the efficiency of the fan and motor cannot be detected in the absence of a measurement of airflow rate.

The supply fan failed to performance as it is manfactured can be further demonstrated on the fan curve plots on Figure 4E. On Figure 4E and 4F, there is one cluster of operation points from supply fan and one cluster of operation points from return fan. The thick black line is the fan curve generated from the catalog data. It is shown that return fan was operated on the fan curve, while the supply fan shifts to the left.

Cooling coil and valve subsystem

Coils and their associated three-way control valves are treated as one subsystem. Coil calibration took three steps. The first step was to match the model with the measured performance data when valve was fully opened under dry coil operation. Coil total UA value was adjusted until both air and water leaving temperatures matched with the measured value. The second step was to calibrate the coil operation at partial wet condition. The ratio of the interior and exterior UA values is adjusted to match data at the partial wet operation, while maintaining the total UA value same as the dry condition. The last step was to calibrate the valve operation. The coil leaving water temperature, the coil entering water temperature, and the mixed return water temperature were used to determine whether the valve was a linear, equal percentage, or quick opening valve and to calculate the polynomial curves to fit it using estimated authority. This method worked well for the experimental data where there was a separate coil leaving water temperature measurement or coil flow rate measurement.

Iowa Energy Center

The model was calibrated with manufacture's catalog data first and then we run the model against the real data collected from the site. Figure 5 is the simulation results of the cooling coil at Iowa Energy Center. The tree way control valve was stepped up from close to fully open, and then down from fully open to fully close. On the airside (Figure 5B), the difference between simulated discharge air temperature and measured discharge air temperature is less than 1 ^{o}F. Figure 5A demonstrats that the installed characteristic of the three-way valve is a quick opening presumably because of the poor authority. The water flow does not change too much after the valve position was higher than 40% because of the poor authority. Figure 5A also shows a hystersis in the control valve. The water flow rate was zero when valve position was 10%. There were water flow only when the valve position reached 20%. Figure 5C shows the X-Yplot of the valve position versus cooling rate of the coil under the steady state. Because of the valve characteristic, the cooling rate is flate after valve position is larger than 40%. The two cooling rate at 20% valve position are caused by hystersis of the valve actuator. The fluctuation of the air temperature is caused by the oscillation of the air flow rate.

Chabot Space and Scientist Musuem

We failed to collet the cooling coil manufacuture's catalog data on site. As in many commerical building, the only information aviable is the cooling coil schedule in the mechanical design drawings. Table 3 has a list of the information avaiable, which is very common in eqiupment schedule. These informaiton is used to calibrate the cooling coil model.

Table 3. Coil Design information in mechanical equipment schedule

CFM	GPM	Water Temp (^oF)		Air Dry Bulb Temp (^oF)		Air Wet Bulb Temp (^oF)	
		Ent	Lvg	Ent	Lvg	Ent	Lvg

•

These information was used to calibrate the model. More specifical, the informate was used to determine the UA values of both water side and air side. After that, the calibrated model was run against the real performance data. Figure 6 shows the results. The test data was collected from EMCS control trends during the normal operation. From the plot, the simulated leaving air temperature is fairly close to the measured supply air temperature, within 2 ^oF. This demonstrates that models calibrated using design information can be useful in passive online monitoring.

SUMMARY AND DISCUSSION (NEED TO BE REWRITE BY PHIL)

A model-based functional testing methodology has been described and demonstrated using measured data. A systematic proceedure for designing active tests has been presented and verified for the case of a mixing box. A software implementation of the model-based analysis procedure detected multiple faults in the mixing box and a model-based analysis detected a fault in an air handling unit fan. On-going work includes an international effort to extent the model library, including the verification of the ability of the models to represent correct operation of real HVAC equipment, and the development of a hybrid approach to fault diagnosis that involves the use of rules to diagnose faults based on the differences between measured behavior and that predicted by a model. The model-based methodology also supports an integrated approach that links design, commissioning and operations, allowing the actual performance of the building and the HVAC system to be tested against the engineering design intent.

In future, certain pre-screening tools to detect some obvious problems need to be developed. It is found out that our tools are overkill for many simple problems in the buildings visited. A pre-screening tool works like a pre filter to detect any obvious problems, such as no control signal or bad sensors, before more sophisticated model based tools is used. A system passed the pre-screening tools will then be subject to model based fault detection. This will save time and allow the fault detection to be implement in more border range of buildings.

The correct thresholds used in the comparator for different components are essential for fault detection. There is strict rule on how much a difference between measured and calculated output can be treated as faults. Currently the threshold is pretty much set up based on the field experience, which can be faulty and unreliable. A tight threshold can trigger false alarms, while a lose threshold may fail to detect faults. An further investigation on the reasonable thresholds that takes account for the simulation and measurement error is necessary for the future work.

Figure 2. Mixing box calibration (ERS)

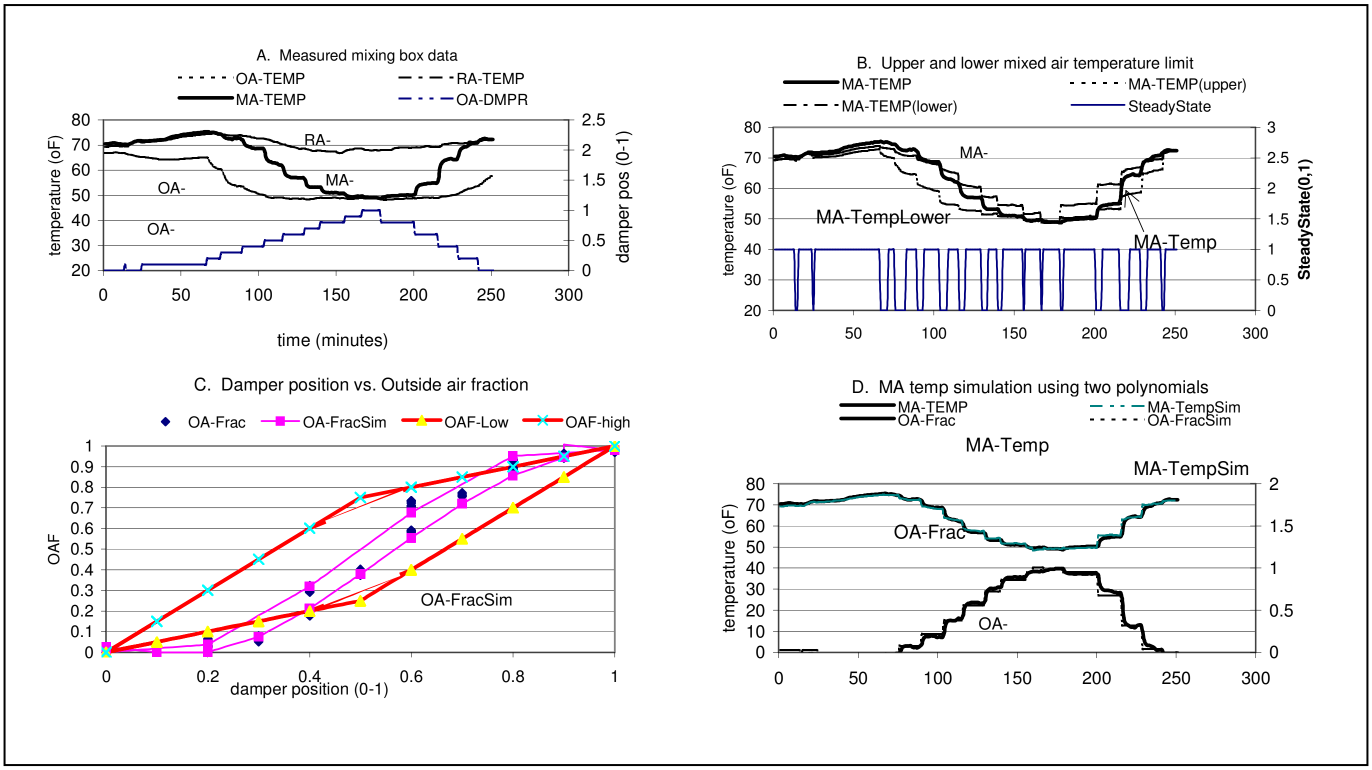

Figure 3. Mixing box fault detection (ERS)

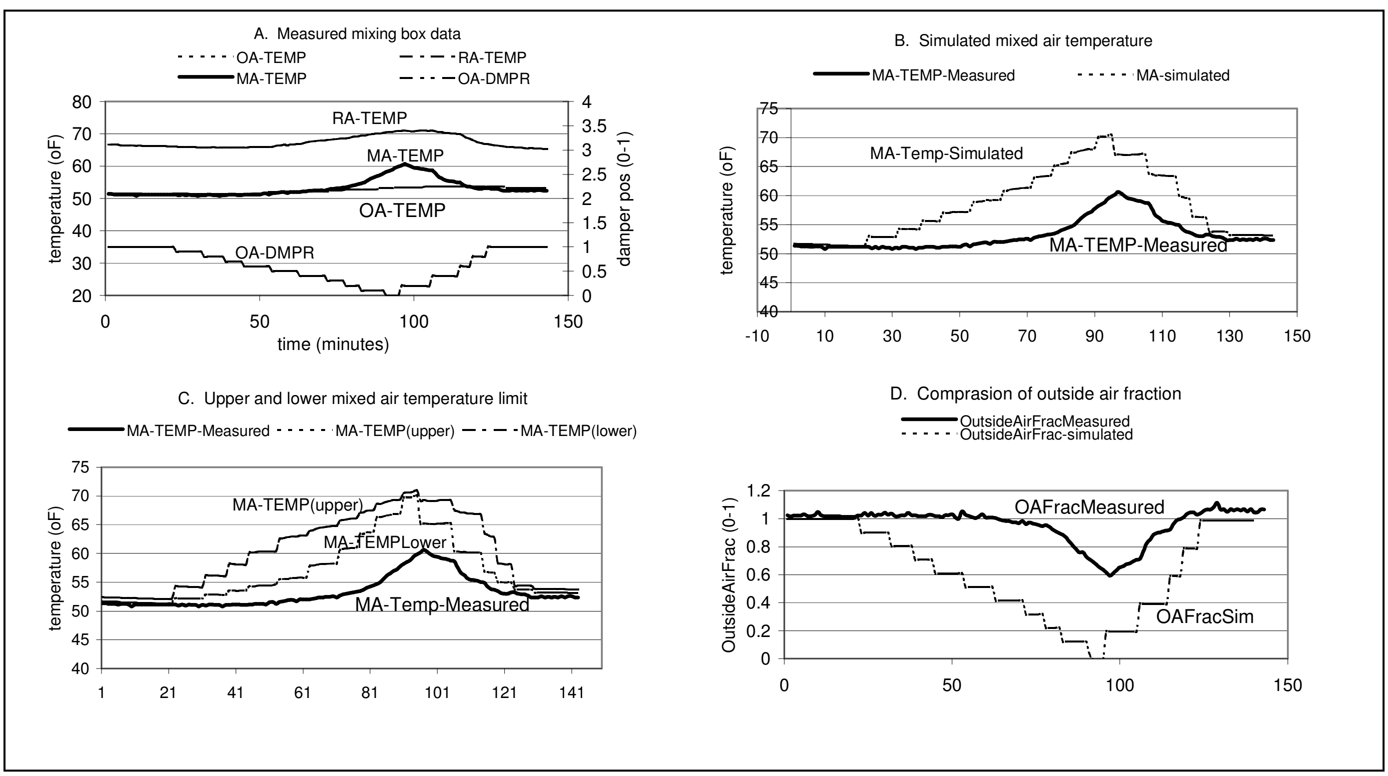

Figure 4. Supply and return fan test (field data)

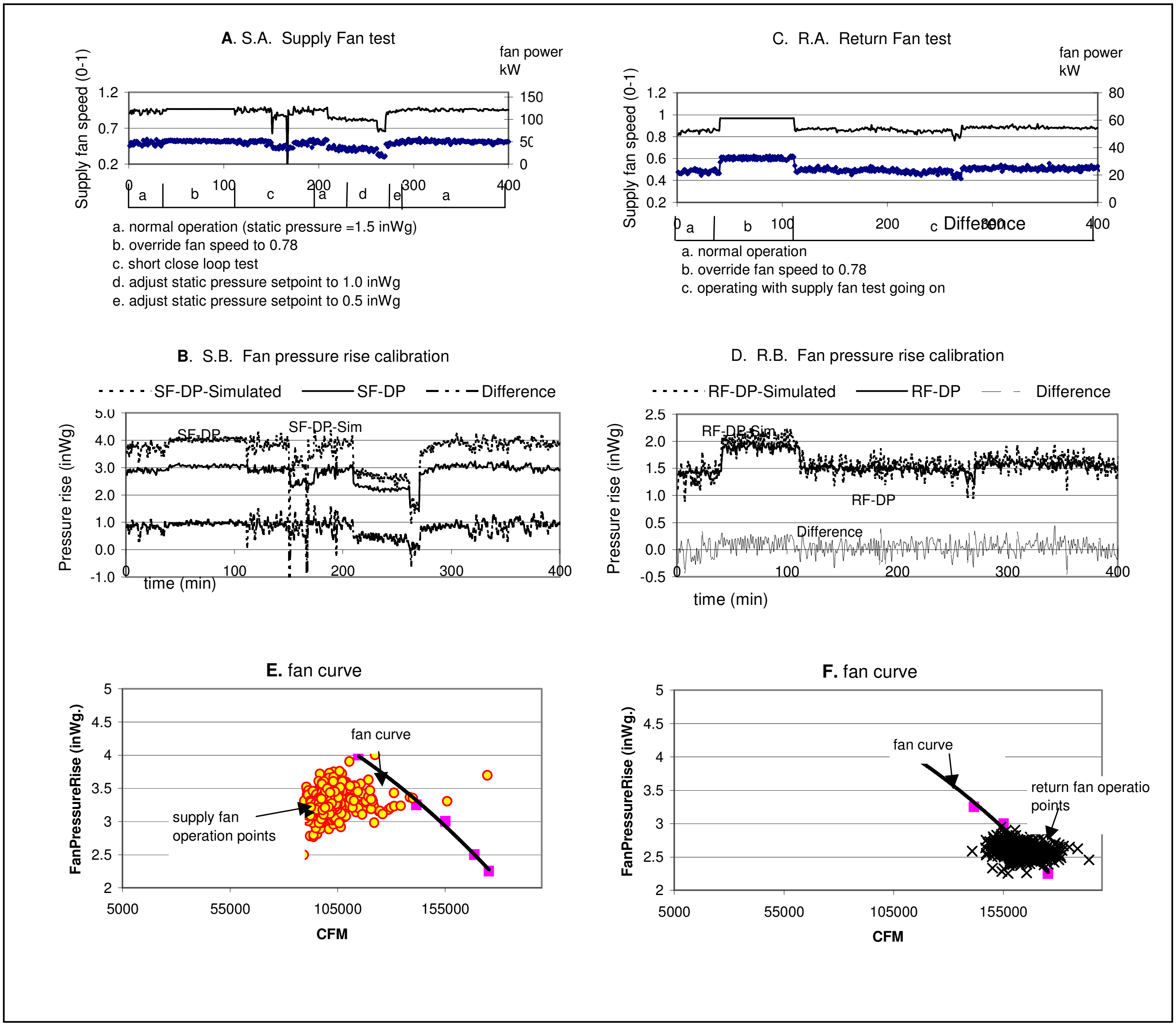

Figure 5 Cooling coil performance (ERS data)

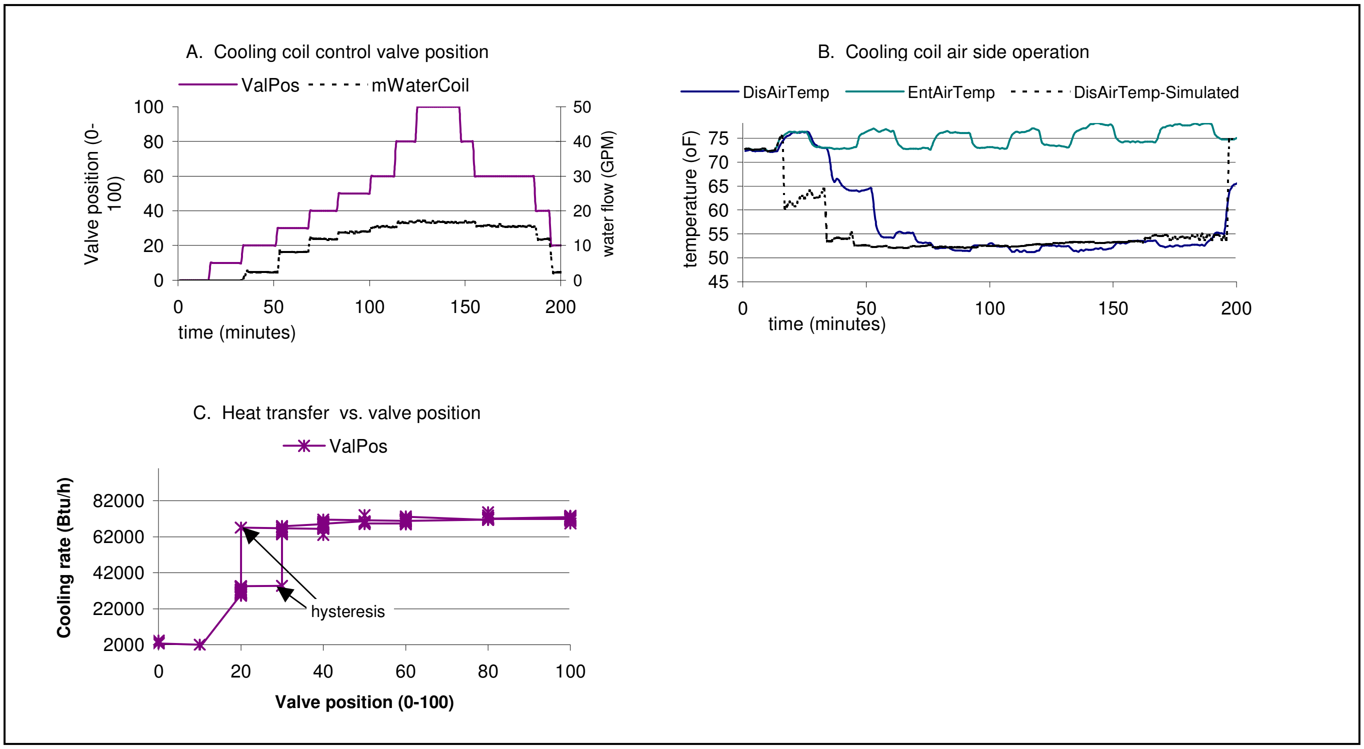

Figure 6 Cooling coil performance (Chabot)

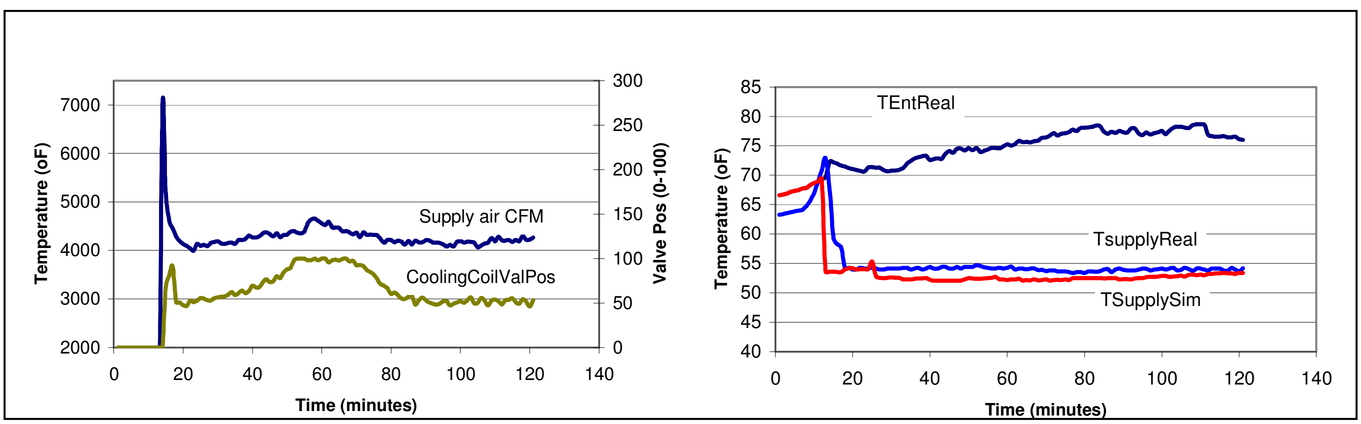

REFERENCES

Brandemuehl, M. J., S. Gabel and I. Andersen. 1993. *A toolkit for secondary HVAC system energy calculations, HVAC2 Toolkit.* Prepared for The American Society of Heating, Refrigerating and Air Conditioning Engineers. TC 4.7 Energy Calculations. Atlanta, GA.: ASHRAE.

Benouarets, M., Dexter, A.L., Fargus, R.S., Haves, P., Salsbury, T.I., and Wright, J.A. 1994. *Model-Based Approaches to Fault Detection and Diagnosis in Air-Conditioning System, Proc. System Simulation in Buildings '94*, Liège, December.

McIntosh I.B.D, Mitchell J.W, Beckman W.A. 2002. *Fault detection and diagnosis in chillers - Part I: Model development and application.* ASHRAE Trans., Vol.106, Part 2, Paper number 4395, 268-282.

Ahn B.C, Mitchell J.W, McIntosh I.B.D. 2001. *Model-based fault detection and diagnosis for cooling towers.* ASHRAE Trans., vol.107, part 1, paper number AT-01-14-1, 839-846,

Haves, P. and Khalsa, S.K. 2000. "Model-based Performance Monitoring: Review of Diagnostic Methods and Chiller Case Study." *Proc. ACEEE Summer Study*, Asilomar, CA, August. LBNL-45949

Hyvarinen, J. 1997. IEA Annex 25 Final Report. VTT, Espoo, Finland.

LBNL. 1999. Proceedings of Diagnostics for Commercial Buildings: From Research to Practice, San Francisco, CA. http://poet.lbl.gov/diagworkshop/proceedings

Xu, Peng and Philip Haves. 2001. *Library of component reference models for fault detection (AHU and chiller).* Report to California Energy Commission. Berkeley, CA.: Lawrence Berkeley National Laboratory.

SPARK. 2002. *Simulation Problem Analyses and Research Kernel.* Lawrence Berkeley National Laboratory and Ayres Sowell Associates, Inc. Berkeley, CA.: Lawrence Berkeley National Laboratory. http://gundog.lbl.gov